

RSC Advances



This is an *Accepted Manuscript*, which has been through the Royal Society of Chemistry peer review process and has been accepted for publication.

Accepted Manuscripts are published online shortly after acceptance, before technical editing, formatting and proof reading. Using this free service, authors can make their results available to the community, in citable form, before we publish the edited article. This *Accepted Manuscript* will be replaced by the edited, formatted and paginated article as soon as this is available.

You can find more information about *Accepted Manuscripts* in the [Information for Authors](#).

Please note that technical editing may introduce minor changes to the text and/or graphics, which may alter content. The journal's standard [Terms & Conditions](#) and the [Ethical guidelines](#) still apply. In no event shall the Royal Society of Chemistry be held responsible for any errors or omissions in this *Accepted Manuscript* or any consequences arising from the use of any information it contains.

**Thermo-responsive triblock copolymer micelles containing
PEG₆₀₀₀ for either water-soluble or water-insoluble drug
sustained release and treatment**

Jun Fu,^b Xinyi Lv^b and Liyan Qiu*^a

^a *Ministry of Education (MOE) Key Laboratory of Macromolecular Synthesis and Functionalization, Department of Polymer Science and Engineering, Zhejiang University, 38 Zheda Road, Hangzhou 310027, China*

^b *College of Pharmaceutical Sciences, Zhejiang University, 866 Yu-Hang-Tang Road, Hangzhou 310058, China*

* Corresponding author. Tel.: +86 571 87952306

E-mail address: lyqiu@zju.edu.cn

ABSTRACT

Improving loading capacity of hydrophobic drug and sustaining release duration of hydrophilic drug is still a big challenge for local drug delivery systems. We synthesized a series of poly(ϵ -caprolactone)-poly(ethylene glycol)-poly(ϵ -caprolactone) triblock copolymers (PCECs) by introducing PEG₆₀₀₀ with relatively higher molecular weight. It was validated that PCECs containing PCL with Mn 1000, 1250, 1350 could form injectable solution via self-assembly and automatically turned into non-flowing gel at physiological temperature. Hydrophobic indomethacin was effectively loaded into PCEC by a modified dialysis method and the anti-inflammation efficacy was maintained for more than 15 days on complete Freund's adjuvant-induced chronic arthritis rats. As for water soluble doxorubicin hydrochloride, just mixed with PCEC, the most significant anti-tumor action against S-180 xenograft tumors in mice with the avoidance of cardiomyocyte damage was achieved during 12-day treatment due to drug sustained release. Therefore, these thermosensitive PCEC polymers have potential superiority for local sustained delivery of hydrophobic or hydrophilic drug.

Keywords: Thermo-sensitive hydrogel; amphiphilic copolymers; sustained release; antitumor; anti-inflammation

1. Introduction

In comparison with intravascular injection which brings drug into a tissue through dense uniform capillary networks, local administration to target tissues is believed to be preferable to a certain extent with remarkable advantages, such as high drug concentration and minimal systemic side effects.¹⁻⁴ Hence, a variety of local drug delivery systems have been recently developed to treat cancers,^{2,5-7} inflammation^{8,9} and cardiovascular disease,¹⁰⁻¹² in forms of implants, microspheres, hydrogel and so on. Among them, local drug delivery systems based on thermo-sensitive polymers have been proven to be more appealing, which undergo phase transition responsive to physiological temperature. Such carriers could be positioned to the target tissue conveniently as an injection and then automatically form a drug depot in situ. As extensively reviewed by several groups,¹³⁻¹⁷ poly(N,N-diethylacrylamide), poloxamers, and block copolymer composed of poly(ethylene glycol) (PEG) and polylactide (PLA) or polycaprolactone (PCL) are considered as classical thermo-sensitive polymers to present a foundation on which many polymer derivatives with specific functions have been designed.^{18,19}

It is well acknowledged that parameters of drug loading capacity and duration of drug release play vital roles in constituting a satisfactory thermo-responsive system for local drug delivery. Currently, the majority of these systems are adopted to load water-soluble substances which can dissolve well into the aqueous polymer solution²⁰⁻²² by pure physical blending force. However, there still exist many problems which seem to be un conspicuous and overlooked, such as drug burst release and short release duration. As reported for thermo-responsive PCL-PEG-PCL hydrogels with low molecular weight PEG₁₀₀₀, the fast release of Vitamin 12 with

nearly 50% amount in 6 h was witnessed.²³ It could be obviously seen that such delivery systems for water-soluble drug fell short of prolonged action effect. On the other hand, the researchers also explored the possibilities of packing hydrophobic drugs by thermo-sensitive gel system.^{24,25} Qiao et al. employed injectable biodegradable temperature-responsive PLGA-PEG₁₅₀₀-PLGA copolymers to pack 5-fluorouracil and indomethacin (IND) with only 0.5% drug loading capacity.²⁶ Furthermore, in pursue of sufficient loading amount for hydrophobic drugs, several researchers adopted an innovative two-step method, by which micelles or particles were first fabricated to load drug and then mixed with polymers. Unfortunately, the preparation procedures turned out to be more tedious.^{27,28} Taken together, extending release duration for hydrophilic drugs and increasing loading content of hydrophobic drugs are still big challenges for researchers to design optimal systems to meet the demand of drug therapy.

With the aim to overcome these problems, we introduced PEG with a relatively higher molecular weight (PEG₆₀₀₀) to the polymer backbone to synthesize a series of triblock PCL-PEG-PCL (PCEC) copolymers. These copolymers displayed thermo-sensitive properties but totally different from that of PEGylated PCL containing low molecular weight PEG.²⁹⁻³² The PCEC in warm solution state can afford to be injected subcutaneously and afterwards transformed to a hydrogel-like drug repository. In addition, they are supposed to form micelles with intermicellar PEG bridges due to long PEG₆₀₀₀ segments, which would facilitate the loading and controlled release of hydrophobic drug and water-soluble drug. Therefore, we adopted IND as a hydrophobic model drug and constructed IND-loaded PCEC system by a modified dialysis method, while doxorubicin hydrochloride (DOX·HCL) as a

water-soluble model drug was mixed with PCEC solution. The drug loading capacity and the corresponding drug release behaviors were evaluated. The pharmacodynamic investigation of drug-loaded systems was carried out using rat chronic inflammation model and S180 xenograft tumors in mice, respectively.

2. Materials and methods

2.1 Materials, cell lines and animals

Polyethylene glycol (PEG₆₀₀₀, Mn=6000), ϵ -caprolactone (ϵ -CL), stannous octoate (Sn(Oct)₂) and DOX·HCL were all purchased from Aldrich. PEG₆₀₀₀ was dried with toluene by azeotropy for several hours to remove trace of water before use. Indomethacin (IND) and Freund's complete adjuvant (CFA) were all purchased from Sigma. Ascitic mouse sarcoma (S180) cell line was bought from Nanjing KeyGEN Biotech. CO., LTD. MTT (3-(4,5-dimethylthiazol-2-yl)-2,5-diphenyl-2H-tetrazolium bromide) was obtained from Sigma–Aldrich (St. Louis, MO, USA; 98% purity). ICR mice weighing 20±2 g and SD rats weighing 180±20 g were purchased from the Laboratory Animal Center of Zhejiang University. The animal care and experimental procedures were conducted according to Institutional Animal Care and Use guidelines.

2.2 Synthesis and characterization of PCEC triblock copolymers

PCEC triblock copolymers were synthesized by ring opening co-polymerization of ϵ -CL using PEG as an initiator and Sn(Oct)₂ as a catalyst. In particular, the calculated amounts of ϵ -CL and 1 wt.% Sn(Oct)₂ were added to 6 g PEG (the feed ratio of

weight: CL/PEG=1/6, 1/3, 5/12, 9/20 and 1/2) under a nitrogen atmosphere and then stirred at 130 °C for 24 h. After cooled to room temperature, the mixture was first dissolved in extreme dry dichloromethane, and then precipitated in excess cold ether. The resultant copolymers were vacuum-dried at ambient temperature. In this paper these polymers are denoted as PCEC_{y-x-y}, where x and y represent the theoretical number average molecular weights (M_n) of the PCL and PEG blocks, respectively.

FT-IR spectra of PCECs were recorded on a NICOLET 200SXV Infrared Spectrophotometer (Nicolet, USA). The molecular weight of PCL was determined by ¹H nuclear magnetic resonance (NMR) in CDCl₃ using an Avence DMX-500 spectrometer (Bruker, Germany) at 400MHZ. Gel permeation chromatography (GPC) (Waters 1525/2414 GPC instrument, Waters refractive index detector, StyragTM HT3 GPC column 300 nm in length and 7.3 mm in diameter, with THF as the mobile phase at a flow rate of 1.0 mL min⁻¹) was used to determine the co-polymer molecular weight and polydispersity ($PDI=M_w/M_n$). The thermal properties of the samples were measured by differential scanning calorimeter (DSC) (NETZSCH 204, NETZSCH, Germany) in a temperature range of -50 to 200 °C at a heating rate of 10 °C min⁻¹.

2.3 Measurement of thermo-responsive property

2.3.1 Gel-sol phase transition behavior

The test of the phase transition behavior was indispensable for the validation of thermo-sensitivity of the copolymers. Each sample at the given concentration was prepared by dissolving the polymer of known amount in the deionized water at a

designated temperature. The volume of the solution was kept at 1 mL in total regardless of the concentration. After being incubated in a water bath at 10 °C for 20 min, the hydrated samples were slowly heated at a rate of 0.5 °C/min, from 10 °C to the temperature at which the solution formed. The gel-sol phase transition diagram of triblock copolymer was recorded using test tube-inverting method with minor modifications.³³ The phase transition was visually observed by inverting the vials, and the conditions of sol and gel were defined as “flow liquid sol” and “no flow solid gel” in 30 s, respectively.

2.3.2 Particle size changes

First, the critical micelle concentration (CMC) of PCEC co-polymers in distilled water was determined by fluorescent spectroscopy (FP-6000, Jasco, Japan) at room temperature using pyrene as a probe according to Ma et al with minor modification.³⁴ The morphology of the copolymer particles in solution was observed by transmission electron microscopy (TEM, JEM-1230, Japan). Then the concentration of various copolymers solution was fixed at 0.5 mg/ml. The particle size was detected by dynamic light scattering (DLS) (Malvern, Nano-S90). The scattering angle was maintained at 90° and the vacuum wavelength was set to 658 nm during all experiments. The detection temperature was from 25 to 70 °C.

2.4 IND-loaded PCEC system

2.4.1 IND loading and release

IND was loaded into PCEC copolymer micelles by the following modified dialysis method. IND and copolymer at weight ratios of 5/100 and 10/100 were dissolved in DMF in a dialysis bag (molecular weight cut-off (MWCO) 3500) and dialyzed against deionized water for 24 h at 70 °C to remove excess DMF. Finally, the solution was filtered and lyophilized to obtain the dry powder of IND-loaded micelles.

The amount of IND loaded in the gels was measured using an ultraviolet spectrophotometer (TU-1800PC, Beijing, China) at a wavelength of 319 nm. It was to be noted that PCEC did not interfere with ultraviolet absorption of IND in the wavelength range 200-400 nm. The drug loading content (LC) was calculated from the mass of incorporated IND divided by that of IND-loaded gels. The drug entrapment efficiency (EE) was defined as the weight percentage of IND in gel relative to the initial feeding amount of IND.

We made minor changes to the membrane model to investigate the release behavior of IND from PCEC micelles *in vitro*. The bottom of a 4 ml Eppendorf tube was cut off and the incision was covered with dialysis membrane (MWCO 3500) as we described before.³⁵ 500 μ L of IND-loaded micelle solution was placed in the 4 ml Eppendorf tube which was further incubated in a 10 ml centrifuge tube of phosphate-buffered saline (PBS) at 37 °C for 12 h with gentle shaking (100 r.p.m.). At the specific time points, the release medium was replaced by fresh PBS and the concentration of IND was determined by ultraviolet spectrophotometry at 319 nm. Each point had three parallel samples and all data were expressed as means \pm SD.

2.4.2 *In vivo* anti-inflammation effect of IND-loaded systems

Adjuvant-induced paw edema model was established to evaluate the anti-inflammation effect of IND-loaded systems. The protocol used was similar to that described by Stein et al.³⁶ with a few modifications. Twenty five male SD rats were randomly divided into five groups: normal saline control, PCEC control and three IND-loaded systems at 4.5 mg/kg drug dose. After incubated in 40 °C shaker for 2 h to avoid the damage to animal tissues, all groups were administered by subcutaneous injection once of 0.1 mL pre-warmed sample solutions. At 1 h post-administration 0.1 ml of CFA was injected subcutaneously into the right back paw to induce inflammation. Then the swelling volume of the rat paws was measured daily by a plethysmometer. In general, the experiment lasted for 15 days. At the end of the experiment, the rats were sacrificed, and their ankle joints were isolated and fixed in 10% neutral-buffered formalin solution and decalcified in a formic acid-formalin solution for 1 week, then embedded in paraffin. Sagittal sections of the ankle joints were stained with hematoxylin and eosin (HE) and were examined under light microscopy.

2.5 DOX·HCL-loaded PCEC system

2.5.1 DOX·HCL loading and release

DOX·HCL-loaded micelles were prepared by physical mixing method. Briefly, DOX·HCL and the copolymer were dissolved in deionized water at 40 °C at weight ratio 10/100. The release behavior was performed as that of IND-loaded system described above. The amount of DOX·HCL was determined with UV-VIS spectrophotometer at 480 nm in PBS solution at pH 7.4.

2.5.2 MTT cell viability assay

We carried out MTT assay to investigate the cytotoxicity of DOX·HCL on S180 cells.³⁷ In view of the special states of PCEC, we only inspected the cytotoxicity of free DOX·HCL on S180 cells. Briefly, S180 cells were seeded on 96-well plate at the density of 2×10^3 cells per well with 100 μ L RPMI 1640 nutrient solution containing 10% FBS at 37 °C in a humidified atmosphere containing 5% CO₂. After 1 day incubation, they were treated with a series of free DOX·HCL solution in different concentration for 1 day. Then 31.5 μ L MTT stock solution was added into each well and incubated for 4 h at 37 °C. After the medium was removed and replaced with 200 μ L dimethylsulfoxide (DMSO), the absorbance measured at 570 nm using the Multiskan MK3 enzyme-linked immunosorbent assay (ELISA) Reader (Thermo, USA). Cell survival was expressed as the percentage of formazan absorbance. The concentrations of DOX·HCL that resulted in 50% of cell death (IC₅₀) in S180 cells were determined from respective dose–response curves. Results were the mean values and standard deviation (SD) from at least three different experiments in triplicate.

2.5.3 *In vivo* antitumor activity of DOX·HCL-loaded systems

24 ICR mice were implanted subcutaneously into right armpit of the mice with S180 ascites tumor cells (about 5×10^6 cells mL⁻¹).³⁸ After tumors volume reached about 100 mm³, the animals were divided at random into 4 groups: normal saline control, PCEC control, free DOX·HCL and DOX·HCL-loaded system at 10 mg/kg drug dose. After incubating all preparations in 40 °C shaker for 2 h to avoid the damage to animal tissues, we separately injected 0.1 mL pre-warmed sample solutions

subcutaneously around the tumors. The tumor diameters in two dimensions and mice body weight were measured every other day in the whole test process. The tumor volume (V) was calculated as $[\text{length} \times (\text{width})^2] / 2$.³⁹ For both free DOX·HCL group and DOX·HCL-loaded system group, one mouse was killed at each determined time point, and the heart, liver, spleen, lung, kidney and tumor were harvested for observation on DOX·HCL fluorescence under Imaging System (CRi maestro EX, USA). And according to the previous study of Li et al.,⁴⁰ the *ex vivo* fluorescence intensity of DOX·HCL in the tumors and major organs was measured and analyzed using commercial software (Maestro software) to semi-quantitatively characterize the biodistribution of DOX·HCL. After the treatments, all mice were killed. From each group tested, we singled out one tumor as well as one heart for histopathological investigation at random. The separated heart and tumor were cut into small pieces and a small portion of them was fixed in formalin and then stained with hematoxylin and eosin (HE). The samples were examined and photographed under an OLYMPAS microscope.

2.6 Statistical analysis

All the data were expressed as means \pm standard deviations (SD). In addition, for comparison, the Student's t-test was introduced between experimental groups and control groups.

3. Results and discussion

3.1 Preparation and characterization of PCEC copolymers

A series of PCL-PEG-PCL triblock copolymers (P1-P5) were prepared by ring-opening polymerization (Table 1). The chemical structure of the PCEC copolymers was characterized by FT-IR, $^1\text{H-NMR}$ and GPC.

Supplementary Fig. 1A shows the FT-IR spectrum of PCEC₁₀₀₀₋₆₀₀₀₋₁₀₀₀. The absorption bands at 1103 cm^{-1} and 1245 cm^{-1} were attributed to the characteristic C-O-C stretching vibrations of the repeated $-\text{OCH}_2\text{CH}_2$ units of PEG and the $-\text{COO}-$ bonds stretching vibrations, respectively. A strong C=O stretching band appeared at 1749 cm^{-1} attributed to the vibrations of the ester carbonyl group. All these signals indicated that PCEC copolymers exhibited characteristic peaks of both PEG and PCL. Since the difference in chain length of PCL block in the five polymers was unobvious, the other PCECs displayed the similar FT-IR characters.

Table 1 The molecular weight and polydispersity of various PCEC copolymers.

Code	copolymer	PCL Mn ^a	Copolymer Mn ^a	Copolymer Mn ^b	PDI ^b
P1	PCL ₅₀₀ -PEG ₆₀₀₀ -PCL ₅₀₀	1009	7009	7932	1.06
P2	PCL ₁₀₀₀ -PEG ₆₀₀₀ -PCL ₁₀₀₀	1989	7989	8975	1.08
P3	PCL ₁₂₅₀ -PEG ₆₀₀₀ -PCL ₁₂₅₀	2547	8574	9708	1.27
P4	PCL ₁₃₅₀ -PEG ₆₀₀₀ -PCL ₁₃₅₀	2807	8807	10135	1.11
P5	PCL ₁₅₀₀ -PEG ₆₀₀₀ -PCL ₁₅₀₀	3186	9186	10570	1.27

^a Molecular weight calculated from $^1\text{H NMR}$ results.

^b Molecular weight calculated from GPC results.

In order to further confirm the formation of PCEC triblock copolymer, $^1\text{H-NMR}$ spectra of $\text{PCEC}_{1000-6000-1000}$ were recorded and shown in supplementary Fig. 1B. The sharp peak at 3.60 was attributed to methylene protons of $-\text{CH}_2\text{CH}_2\text{O}-$ in PEG block. Peaks at 1.35, 1.62, 2.30, and 4.06 ppm were assigned to methylene protons of $-(\text{CH}_2)_3-$, $-\text{OCCH}_2-$, and $-\text{CH}_2\text{OOC}-$ in PCL blocks, respectively. The very weak peaks at 4.23 and 3.82 ppm were attributed to methylene protons of $-\text{O}-\text{CH}_2-\text{CH}_2-$ in PEG end block that linked with PCL blocks, respectively. The number-average molecular weight of PCEC block copolymers was calculated from $^1\text{H-NMR}$ spectra by comparing the integral intensities of peaks at about 4.23 (d) and 4.06 (a) ppm. The results were consistent with the theoretical values calculated from the feed ratio and the values measured by GPC (Table 1).

DSC measurement was also employed to verify the structure of copolymers. During the heating process, one melting peak at 50-55 °C was observed (Supplementary Fig. 1C), which was attributed to the melting of crystallized PCL domains. This phenomenon was similar to the endothermic peaks of a multiblock PEG-PCL copolymer consisting of low-molecular-weight PEG and PCL during the heating process.^{41,42} Therefore, it could be concluded that the copolymers contained PCL block.

All these data integrately demonstrated that the PCEC copolymers with PEG_{6000} and different amount of PCL had been successfully synthesized.

3.2 Gel-sol phase transition

As several papers reported, PCL-PEG-PCL tri-block copolymers containing low molecular weight PEG displayed thermo-sensitivity properties with sol-gel-sol three-phase transition.³⁰ The gelation mechanism might be micelle packing driven by hydrophobic interactions, as well as partial crystallization of PCL blocks. However, once increasing the length of PEG segments to 6000 in PCEC, the thermo-sensitivity notably changed to gel-sol two-phase transition. At a relatively low temperature, the copolymer solution was capable of forming gel, while with the temperature increasing, the polymer hydrogel would convert to solution. The temperature at which gel-sol transition occurred was defined as critical gelation temperature (CGT) of polymers. In this paper, we aimed to construct an injectable thermo-sensitive carrier for drug local sustained delivery, therefore the appropriate CGT should be set over 37 °C but not exceed 43 °C to prevent heat hurt.

It was observed that phase transition behavior of PCEC aqueous solutions was closely related to the polymer chemical structure and solution concentration. P1 solution couldn't form hydrogel at 10 °C even the mass fraction in water was up to 25 wt%, namely there wasn't any CGT for P1. When it came to P5 with strong hydrophobicity, its solution became very sticky at 12 wt% concentration but the precipitation occurred when the temperature increased to 45 °C without the gel-sol transition process. Hence, P1 and P5 were not applicable for this study.

Fig. 1A manifested the phase transition behavior of the other three PCECs. For P2, the CGTs fell within the range of 35~55 °C with the corresponding solution concentration of 20~30 wt%, indicating that the higher solution concentration, the higher CGT. Herein, 20 wt% was defined as a critical gel concentration (CGC) of P2 in this typical phase diagram. The similar phenomenon was observed for P3 and P4. It

was found that CGC and CGT were mainly determined by the PEG/PCL block ratio. With decreasing PEG/PCL block ratio, the CGC decreased and CGT was elevated on account of the enhanced hydrophobicity of the polymer. Fig. 1B intuitively reflected the state of different PCEC copolymers at the certain concentration with temperature increasing from 25 °C to 52 °C.

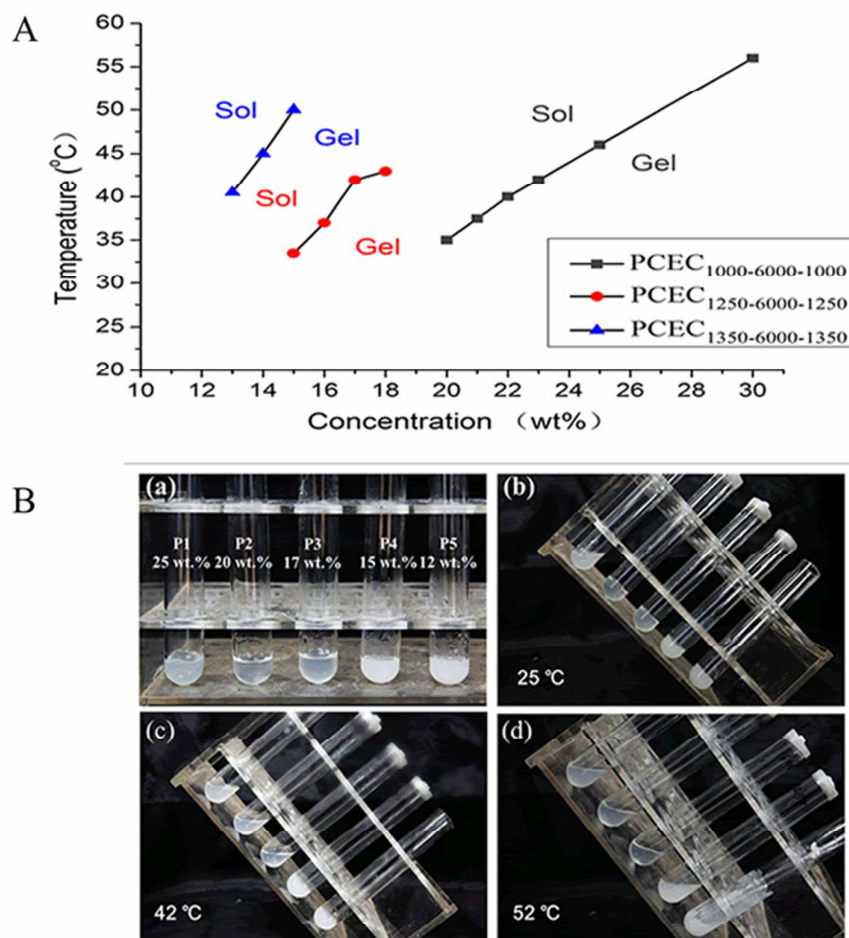


Fig. 1 (A) The gel-sol transition diagram of PCEC copolymers and (B) their gel-sol phase transition behavior tested by the tube-inverting method at various temperatures.

P1: PCEC₅₀₀₋₆₀₀₀₋₅₀₀ (25 wt%); P2: PCEC₁₀₀₀₋₆₀₀₀₋₁₀₀₀ (20 wt%); P3: PCEC₁₂₅₀₋₆₀₀₀₋₁₂₅₀ (17wt%); P4: PCEC₁₃₅₀₋₆₀₀₀₋₁₃₅₀ (15 wt%); P5: PCEC₁₅₀₀₋₆₀₀₀₋₁₅₀₀ (12 wt%).

3.3 Micellization behavior of PCEC in water

To validate the micellization behavior of these novel amphiphilic PCECs (P2, P3, P4), we determined their CMC values in aqueous solution. Taking P2 as an example, supplementary Fig. 2A shows the fluorescence intensity of pyrene increased with increasing polymer concentration, and the characteristic band of pyrene shifted from 333 to 338 nm. This change indicated that pyrene molecules transferred from polar water medium to the hydrophobic core of micelles. The CMC value of polymer can be calculated from the curve drawn by the intensity ratios (I_{338}/I_{333}) as a function of polymer concentration (supplementary Fig. 2B). Therefore, the CMC values of P2, P3, P4 were 6.35×10^{-3} mg/ml, 2.54×10^{-3} mg/ml and 3.53×10^{-3} mg/ml, respectively, indicating that these three PCECs could self-assemble into nanoparticles in water. As shown in supplementary Fig. 3, these nanoparticles all displayed homogeneous spheres outline and the particle size was increased when increasing molecular weight of PCL block.

3.4 Particle size change responsive to temperature

To further explore the gel transition mechanism of PCEC, the size changes of PCEC self-assemblies under different temperatures were investigated. The concentration of polymer solution was set at 0.5 mg/ml, which was over CMC to guarantee the formation of self-assembled micelles. The results shown in Fig. 2 demonstrated that the PCEC could simultaneously self-assemble to two batches of particles with small size (20-30 nm) and large size (150-350 nm), respectively. At room temperature the proportion of small size particles was low while that of large size particles was high.

However, with the rise of temperature, the proportion of small size particles increased gradually accompanied with the proportion reduction of large size particles. For instance, the proportion of P2 batch 1 (small size) increased from 41.8% to 79.3%, while that of batch 2 (big size) reduced from 58.2% to 20.7% with the increase of temperature from 25 °C to 70 °C, demonstrating the automatic size variation of self-assembled nanoparticles responsive to the increased temperature.

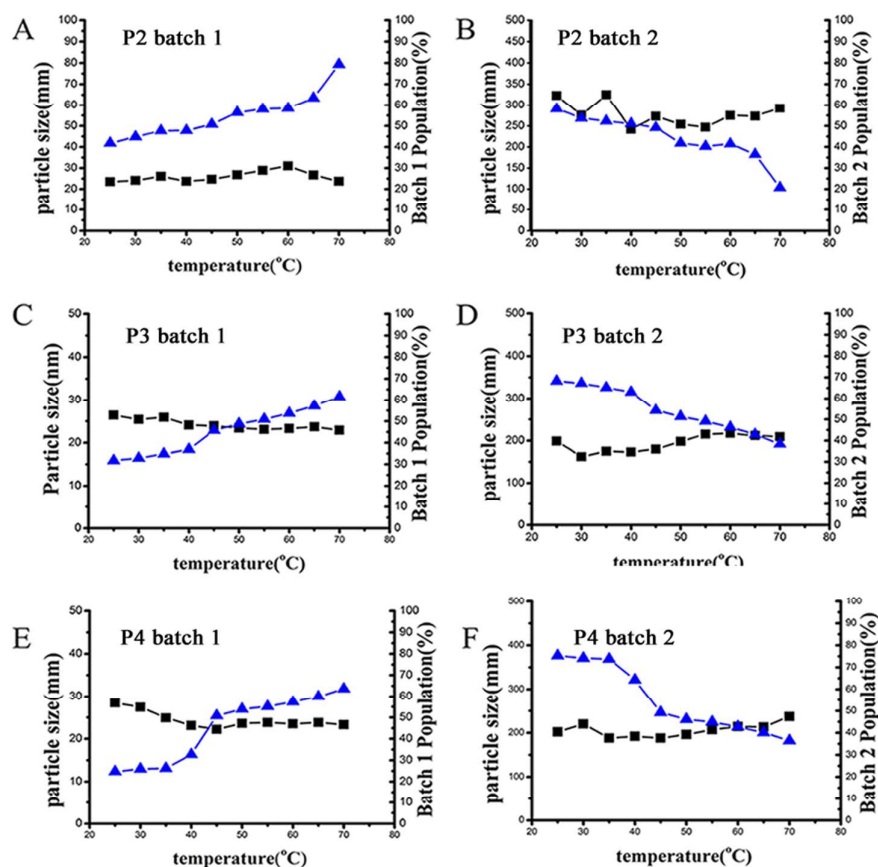


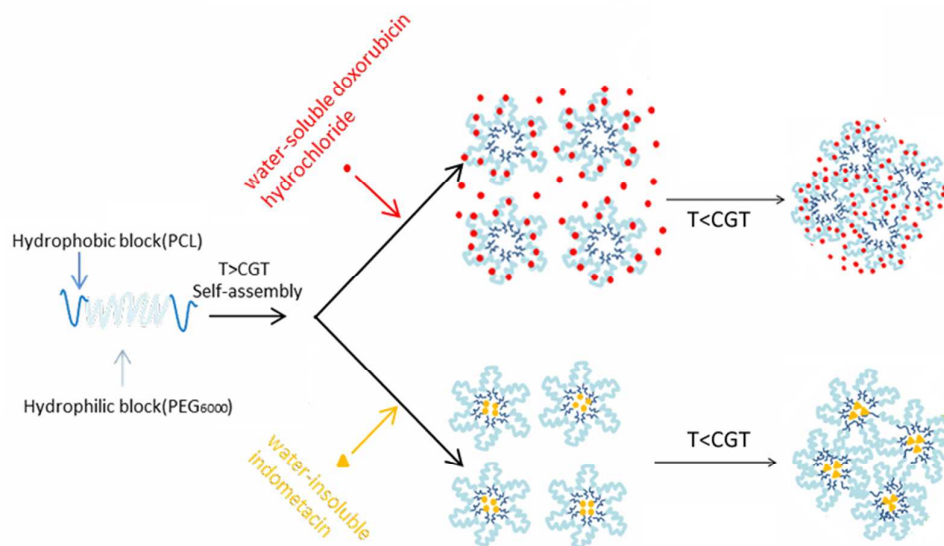
Fig. 2 The particle size and proportion change of three self-assembled PCECs in water vs. the temperatures. (A) PCEC₁₀₀₀₋₆₀₀₀₋₁₀₀₀ batch 1; (B) PCEC₁₀₀₀₋₆₀₀₀₋₁₀₀₀ batch 2; (C) PCEC₁₂₅₀₋₆₀₀₀₋₁₂₅₀ batch 1; (D) PCEC₁₂₅₀₋₆₀₀₀₋₁₂₅₀ batch 2; (E) PCEC₁₃₅₀₋₆₀₀₀₋₁₃₅₀ batch 1; (F) PCEC₁₃₅₀₋₆₀₀₀₋₁₃₅₀ batch 2. ▲ represents the proportion, ■ represents the particle size.

Based on the results shown in Fig. 1 and Fig. 2, the phase transition mechanism of PCECs was explained as follows. At the lower temperature, once the copolymer concentration was up to a certain value (CGC), micelle clusters with relatively big size gathered to form gel, where relatively long PEG chains looped out of the micelle and formed bridge bonds with other micelles. At the temperature rose over CGT, however, the big micelle clusters would disperse into small single one probably due to the active chain motion and the breakage of intermicellar PEG bridge bonds, which triggered the phase transition from gel to solution of the system.

3.5 IND-loaded PCEC system

3.5.1 IND loading and release

As illustrated above, the copolymer P2, P3 and P4 dissolved in water as micelles at higher temperature ($T > \text{CGT}$), which was in favor of drug loading homogeneously. Therefore, IND can be loaded into PCEC micelles by dialysis method at 70 °C via hydrophobic interaction between drug and PCL blocks. The mechanism of IND-loading was displayed in Scheme 1 that IND were mostly encapsuled in the hydrophobic core of PCEC micelles. As listed in Table 2, the LC of IND increased with the increase of drug feeding, and the EE of each copolymer system was above 80 % under different feed ratios. IND is a hydrophobic substance with poor solubility in water of only 4×10^{-3} mg/ml,²⁵ but the concentration of IND in 25 wt% IND-P2-DSA solution reached 14.16 mg/mL, which was 3540 times increase in solubility. Consequently, the solubility of IND was significantly enhanced to meet the requirement of clinical administration as an injection.



Scheme 1. The drug-loading mechanism of thermo-sensitive PCEC systems for water-insoluble indomethacine and water-soluble doxorubicin chloride.

Table 2 The EE and LC of IND-loaded copolymer systems.

Code	Copolymer	Drug/Copolymer feed ratio (mg/mg)	LC (%)	EE (%)
IND-P2-DS	PCL ₁₀₀₀ -PEG ₆₀₀₀ -PCL ₁₀₀₀	5/100	4.25±0.18	81.3±3.9
IND-P2-DS	PCL ₁₀₀₀ -PEG ₆₀₀₀ -PCL ₁₀₀₀	10/100	9.28±0.17	92.1±1.8
IND-P3-DS	PCL ₁₂₅₀ -PEG ₆₀₀₀ -PCL ₁₂₅₀	5/100	4.46±0.33	83.7±6.9
IND-P4-DS	PCL ₁₃₅₀ -PEG ₆₀₀₀ -PCL ₁₃₅₀	5/100	4.65±0.41	87.5±8.5
IND-P4-DS	PCL ₁₃₅₀ -PEG ₆₀₀₀ -PCL ₁₃₅₀	10/100	9.03±0.23	89.4±4.8

The *in vitro* release behavior of IND from PCEC hydrogel was studied and the results were shown in Fig. 3A. The released amount of IND from P2-DS, P3-DS, P4-DS were only 1.59%, 1.58% and 1.56% in the first 1 h, respectively,

demonstrating no obvious drug burst release. During the following days, IND was released from PCEC hydrogel in a sustained manner. Furthermore, the length of PCL segment in the copolymer brought a dominant effect on the release profile of IND. The longer PCL segment, the slower IND released. After 15 d, drug release amount of IND-P2-DS and IND-P3-DS were 96.0% and 96.0%, respectively, whereas that of IND-P4-DS was only 74.1%.

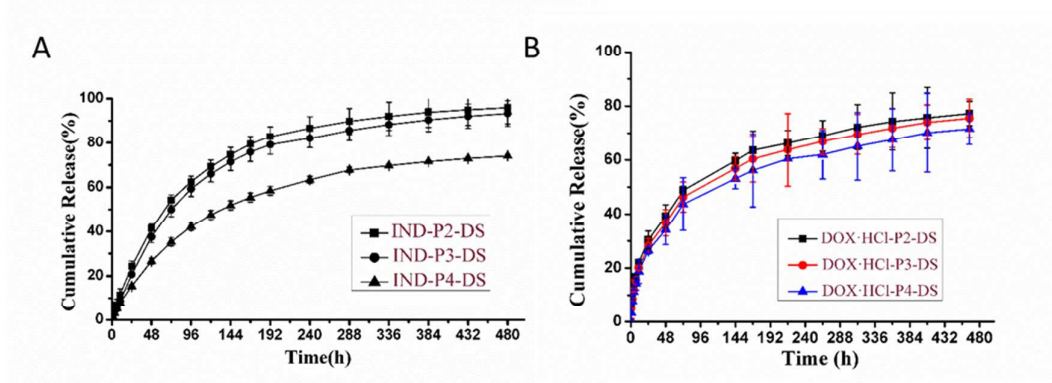


Fig. 3. *In vitro* drug release behavior of drug-loaded copolymer systems. (A) IND-loaded system and (B) DOX·HCL-loaded systems.

3.5.2 Therapeutic effect of IND-loaded PCEC in arthritis rat model

We examined the effects IND-loaded PCEC treatment on the oedema induced by complete Freund's adjuvant with 5 rats in each group. The results demonstrated that prophylactic treatment of IND-loaded PCEC (4.5 mg/kg) markedly inhibited the oedema induced by CFA. One day after the treatment, comparing the control group with IND-loaded copolymer solution, the rat paw volume of IND-P2-DS was smaller and the inhibition of inflammation could last for 7 days or so. The anti-inflammation efficacy of IND-P3-DS was similar to that of IND-P2-DS. Fig. 4A indicated that after

IND-P4-DS was administrated, the volume of rat paw was maintained at a relatively low level during the treatment period of 15 days. And during the experiment, we could see clearly that the paw swelling in two control groups were much worse than that of IND-P4-DS, even the center of the paw emerged pus.

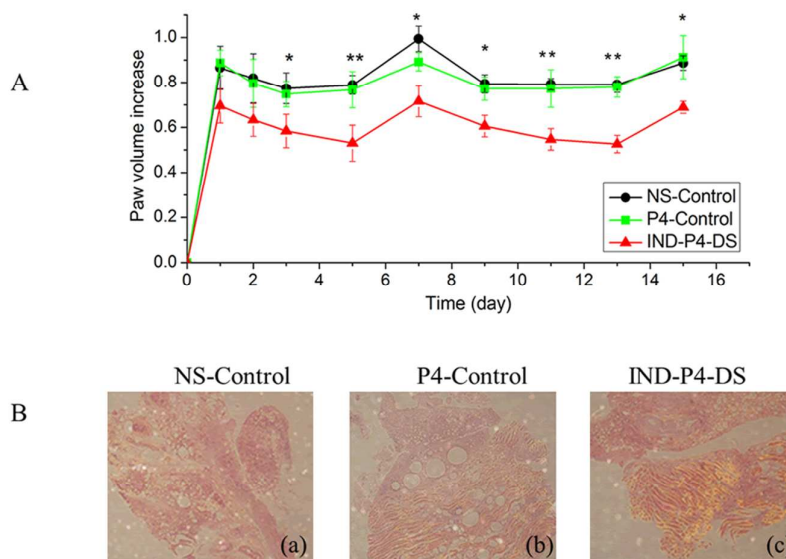


Fig. 4 (A) Anti-inflammation effect of normal saline control, P4 control and IND-P4-DS at 4.5 mg/kg drug dose in Freund's adjuvant-induced arthritis model. (* $p < 0.05$, ** $p < 0.01$ vs NS-control). (B) The tissue sections of ankle joints in arthritis rat treated with saline control, P4 control, IND-P4 drug loaded system.

After rats paw swelling chronic inflammation experiment for IND-P4-DS was finished on the fifteenth day, the histologic examination of their ankle joints were performed. As shown in Fig. 4B (a) and (b), in normal saline and blank polymer groups, sarcoplasm was gathered and a large number of inflammatory cells infiltrated. The cells arranged paralleling to the long axis of myofibril edema distinctly. Especially the paw's normal long cylindrical multi-core skeletal muscle fibers cells

were absent. In contrast to these pathological changes in the modal rat, the muscle fiber of rats treated with IND-P4-DS arranged closely with dozens of oval nucleus, little dyeing and rich muscle blade nucleus, and a few of edema (Fig. 4B (c)). This result revealed that IND released slowly from PCEC₁₃₅₀₋₆₀₀₀₋₁₃₅₀ in rats exerted a pronounced sustained anti-inflammatory effect.

3.6 DOX·HCL-loaded PCEC systems

3.6.1 DOX·HCL loading and release

Since DOX·HCL is water soluble, so it was quite easy to prepare drug-loaded PCEC system just by dissolving them together in water. As shown in Scheme 1, DOX·HCL were distributed in the tangled textures of PEG blocks rather than hydrophobic PCL cores like IND. Therefore, Fig. 3B shows that DOX·HCL release can be well sustained for 12 days without any obvious burst release, and there was no significant difference in the release profiles among three copolymers. On the 12th day, the cumulative release of DOX·HCL were 70.12%, 68.44%, and 64.02% for three copolymers, respectively. To illustrate the significance of PEG₆₀₀₀ for drug controlled release, we synthesized PCEC₁₀₀₀₋₁₀₀₀₋₁₀₀₀ with the same length of PCL as that of PCEC₁₀₀₀₋₆₀₀₀₋₁₀₀₀ and the shorter length of PEG, and investigated its drug release behavior. As shown in Supplementary Fig. 5, the burst drug release from PCEC₁₀₀₀₋₁₀₀₀₋₁₀₀₀ system was serious that the cumulative release was up to 70.6% in the first 24 h, much larger than that of PCEC₁₀₀₀₋₆₀₀₀₋₁₀₀₀ (30.3%). Since PEG₁₀₀₀ segment is much shorter than PEG₆₀₀₀, PCEC₁₀₀₀₋₁₀₀₀₋₁₀₀₀ hydrogel was composed of independent micelles which packed together without intermicellar PEG bridges.

Consequently, water soluble DOX·HCL was mainly located in the gap between micelles, which resulted in the drug burst release.

3.6.2 Biodistribution and anti-tumor effect of DOX·HCL

DOX·HCL is a highly effective anti-neoplastic agent to treat several adult and pediatric solid tumors, leukemia, and lymphomas. However, the successful application of DOX·HCL has been hampered by toxicities such as hematopoietic suppression, nausea, vomiting, extravasation, and alopecia, yet the most feared side-effect is cardiotoxicity.^{43,44}

To investigate the drug distribution in the body, *ex vitro* fluorescence experiment was conducted since the fluorescence intensity values of DOX·HCL is correlated with its concentration. Mice bearing S180 tumors were intratumorally injected with free DOX·HCL solution and DOX·HCL-P4-DS solution at the drug dose of 10 mg/kg when the tumor volumes researched $\sim 100 \text{ mm}^3$. A comparison of drug fluorescence in tumors and other normal tissues after injection at six chosen time points and the semi-quantitative analysis of fluorescence intensity are illustrated in Fig. 5. After administration of either free DOX·HCL solution or DOX·HCL-P4-DS, liver and kidney showed a substantial accumulation amount of DOX·HCL, which may induce systemic toxicity and led to the weight loss of mice. For free DOX·HCL group, the drug level at tumor was high in 2 h, and after that DOX·HCL was cleared fast and the average fluorescence intensity was decreased to 58.73 at 72 h (Fig. 5B). However, compared with free DOX·HCL group, the drug amount in DOX·HCL-P4-DS group declined significantly more slowly. The fluorescence can be still observed after 48 h

(Fig. 5A) and the corresponding fluorescence intensity was kept at 114.75, which was 1.95-fold higher than that of free DOX·HCL group (Fig. 5C). These results reflected the stability of micelles and extended drug retention time at tumor site, which was benefit to the sustained tumor inhibition effect.

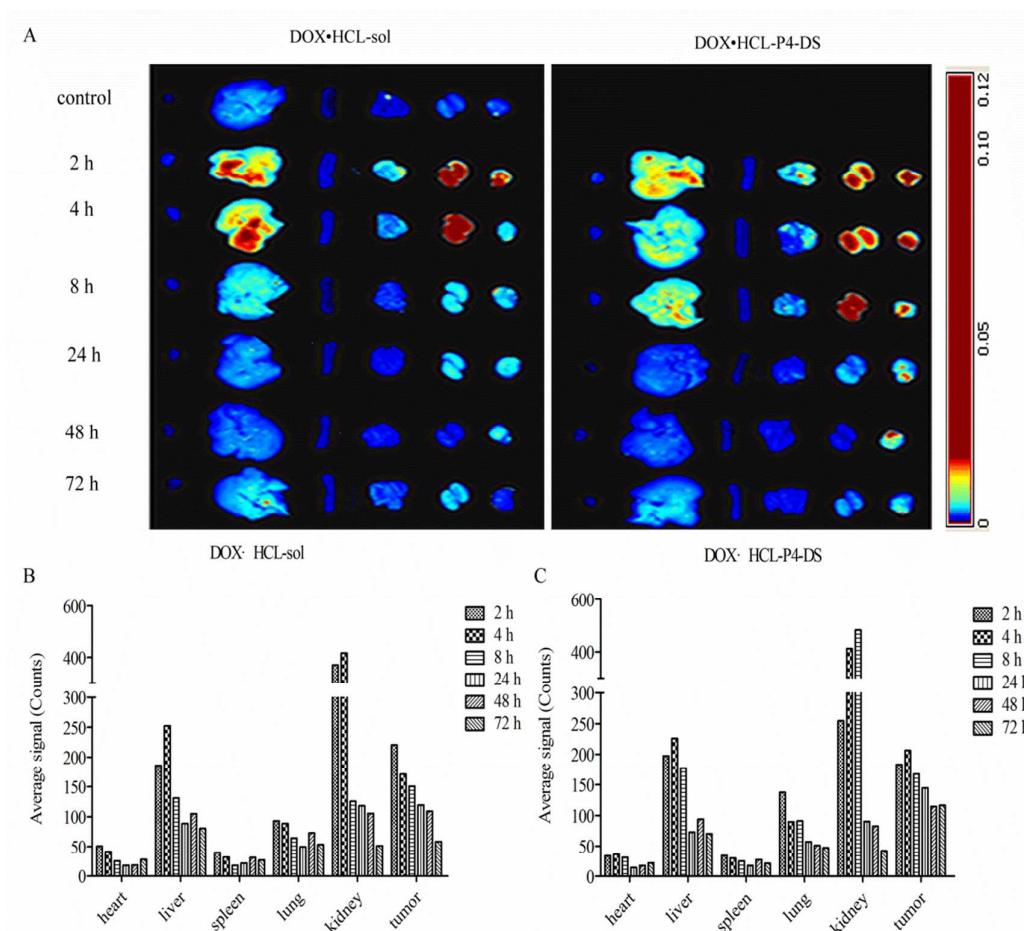


Fig. 5 (A) The *ex vivo* fluorescence images at heart, liver, spleen, lung, kidney and tumor figure of free DOX·HCL (single dose at 10 mg/kg) and DOX·HCL-P4 drug loaded system groups (single dose at 10 mg/kg) at the various time points after injection, and the average signals collected from the major organs (heart, liver, spleen, lung and kidney) and tumor at different time points in mice bearing S180 tumors after the treatment of (B) DOX·HCL-sol and (C) DOX·HCL-P4-DS.

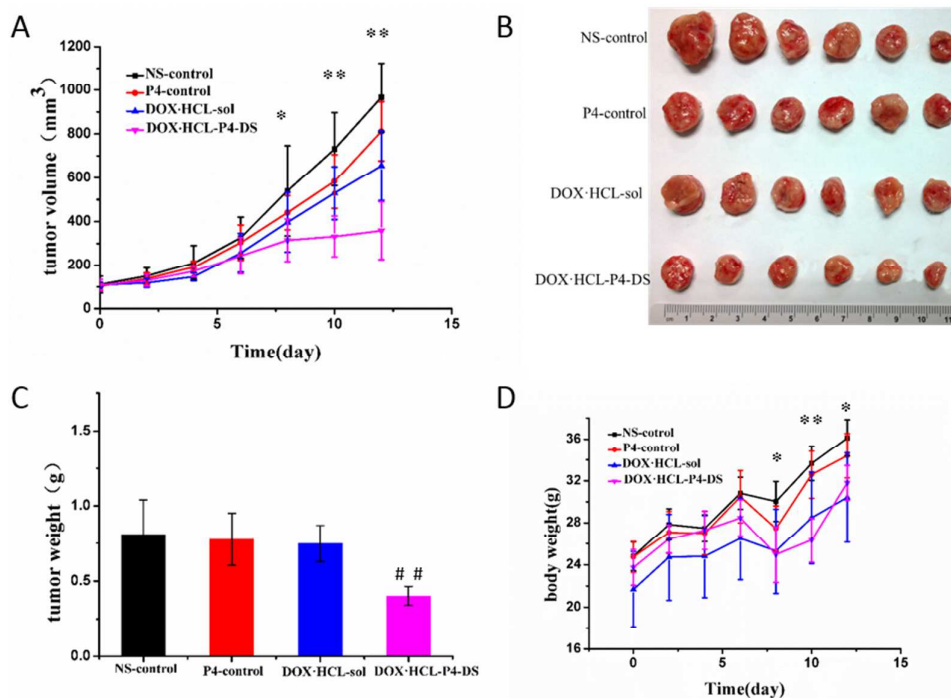


Fig. 6 Inhibition of tumor growth by subcutaneous injection around tumors of normal saline, P4 control, free DOX·HCL or DOX·HCL-P4 drug loaded system at 10 mg/kg drug dose. (A) Curve of tumor inhibition; (B) Tumor photos; (C) Tumor weight; (D) Body weight of animal. (* $p < 0.05$ vs NS-control, ** $p < 0.01$ vs NS-control, ## $p < 0.01$ vs DOX·HCL-sol)

For antitumor effect evaluation, mice bearing S180 tumors were intratumorally injected with 0.1 mL normal saline, P4 solution, free DOX·HCL solution (10 mg/kg) and DOX·HCL-P4-DS solution (10 mg/kg) when the tumor volumes researched ~ 100 mm³. Within 6 days after administration, there was no significant difference of therapeutic effects among the four groups (Fig. 6A). However, 6 days later, the tumor growth of DOX·HCL-P4-DS group became much slower than that of mice treated with normal saline, P4 solution or free DOX·HCL, and this difference became more

significant after 8 d. On one hand, according to the MTT assay, the IC_{50} of free DOX·HCL is $4.296 \pm 0.3459 \mu\text{g/ml}$, indicating S180 cells are insensitive to DOX·HCL. On the other hand, free DOX·HCL was eliminated too quickly as shown in Fig. 5 to exert satisfactory anti-tumor effect. On 12 d, the mice were sacrificed and the tumors were isolated and weighed. The mean tumor weight of normal saline, P4 control, free DOX·HCL groups were 0.81 g, 0.777 g, 0.75 g, respectively, which was significantly larger than that of DOX·HCL-P4-DS group (0.403 g) (Fig. 6B and C).

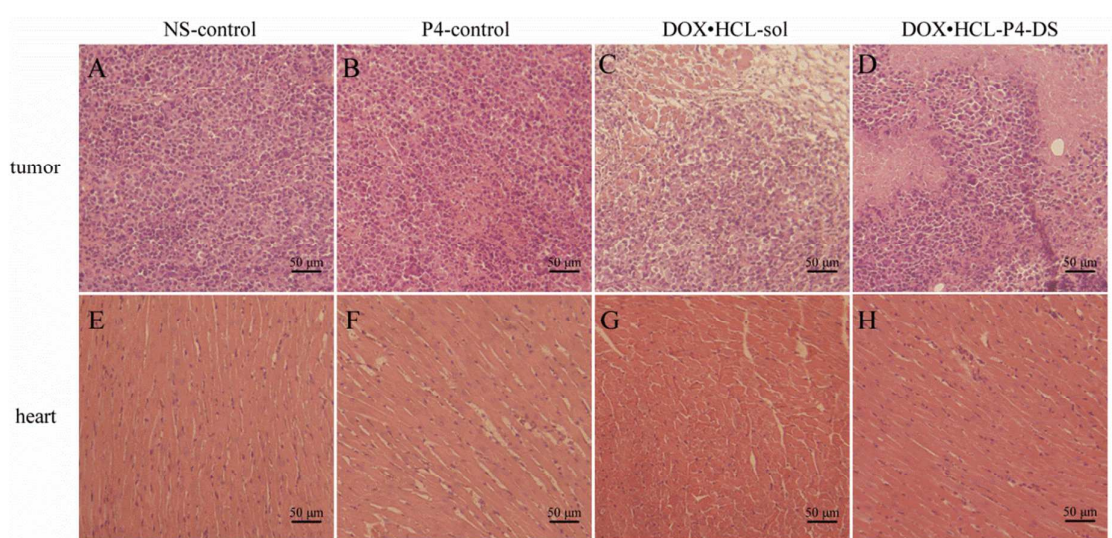


Fig. 7 Histologic evaluation of tissues from mice treated with normal saline control, P4 control, free DOX·HCL (single dose at 10 mg/kg), and DOX·HCL-P4 drug loaded system (single dose at 10 mg DOX·HCL/kg). Bar, 50 μm .

The antitumor efficacy of DOX·HCL-P4-DS were further analyzed by histological examination. Hematoxylin/eosin (HE) staining showed that the tumors treated with normal saline and P4 control typically consisted of tightly packed tumor cells and some necrotic regions because of rapid tumor growth. However, extensive nuclear shrinkage and fragmentation were observed in the tumors which were treated by free

DOX·HCL solution and DOX·HCL-P4-DS (Fig. 7A-D). Compared with the group of free DOX·HCL solution, the tumors in DOX·HCL-P4-DS group contained a much larger proportion of necrotic regions, indicating stronger inhibition effect on tumor growth.

During the anti-tumor treatment, the loss of mouse body weight was found for free DOX·HCL solution and DOX·HCL-P4-DS groups (Fig. 6D). Fortunately, a few days later the weight of mice recovered to normal level. Irreversible cardiotoxicity due to cardiomyocyte damage is a common side effect of DOX·HCL. To evaluate whether the myocardial damage was induced by the DOX·HCL-P4-DS treatments, the histological changes of cardiomyocytes were examined by light microscopy. As shown in Fig. 7E-H, the free DOX·HCL solution-treated group exhibited severe myocardial damage with disorganized myofibrillar arrays. For DOX·HCL-P4-DS groups, however, the compact cardiomyocytes lined up in order with clear structures similar to normal ones shown in normal saline- and P4-treated groups. These results indicated that due to the slow drug release rate of DOX·HCL-P4-DS, the systemic absorption of DOX·HCL was effectively inhibited, which finally avoided the common side effects on heart of DOX·HCL.

4 . Conclusion

This study focused on PEG₆₀₀₀ for ring-opening polymerization of CL and optimized the ratio of hydrophilic/hydrophobic chain to obtain a series of thermo-responsive PCL-PEG₆₀₀₀-PCL copolymers with appropriate gel-sol transition character for local drug delivery. In general, these copolymers demonstrated extraordinary solubilization

effect for hydrophobic IND and sustained release of both hydrophobic IND and water-soluble DOX·HCL. Therefore, the advantages of PCEC copolymers used *in vivo* were highlighted including prolonged anti-inflammatory or anti-tumor treatment efficacy and minimized systemic side effect.

Acknowledgments

This work was financially supported by National Natural Science Funds for Excellent Young Scholar (81222047) and the Ministry of Education Program for New Century Excellent Talents (NCET-11-0454).

References

1. A. Rösler, G. W. Vandermeulen, H.-A. Klok, *Adv. Drug Deliv. Rev.*, 2012, **64**, 270.
2. J. B. Wolinsky, Y. L. Colson, M. W. Grinstaff, *J. Control. Release*, 2012, **159**, 14.
3. M. Vallet-Regí, F. Balas, M. Colilla, M. Manzano, *Prog. Solid State Chem.*, 2008, **36**, 163.
4. T. M. Allen, P. R. Cullis, *Adv. Drug Deliv. Rev.*, 2013, **65**, 36.
5. K. Gulati, M. S. Aw, D. Losic, *Int. J. Nanomedic.*, 2012, **7**, 2069.
6. T. A. Juratli, G. Schackert, D. Krex, *Pharmacol. Ther.*, 2013, **139**, 341.
7. S. K. Mouli, P. Tyler, J. L. McDevitt, A. C. Eifler, Y. Guo, J. Nicolai, R. J. Lewandowski, W. Li, D. Procissi, R. K. Ryu, *ACS nano*, 2013, **7**, 7724.
8. M. Bassetti, D. Schär, B. Wicki, S. Eick, C. A. Ramseier, N. B. Arweiler, A. Sculean, G. E. Salvi, *Clin. Oral Implants Res.*, 2013, **24**, 104.
9. H. Inoue, Y. Arai, T. Kishida, M. Shin-Ya, R. Terauchi, S. Nakagawa, M. Saito, S. Tsuchida, A. Inoue, T. Shirai, *Ultrasonics*, 2014, **54**, 874.
10. K. L. Kennedy, A. R. Lucas, W. Wan, *Curr. Drug Delivery*, 2011, **8**, 534.

11. M. Y. Maslov, E. R. Edelman, A. E. Wei, M. J. Pezone, M. A. Lovich, *J. Control. Release*, 2013, **171**, 201.
12. U. Speck, B. Scheller, W. Rutsch, M. Laule, V. Stangl, *Eur. J. EuroPCR Collab. Working Group Int. Cardiology Eur. Soc. Cardio*, 2011, **7**, K17.
13. E. Ruel-Gariepy, J. C. Leroux, *Eur. J. Pharm. Biopharm.*, 2004, **58**, 409.
14. Y. Tang, C. L. Heaysman, S. Willis, A. L. Lewis, *Expert Opin. Drug Deliv.*, 2011, **8**, 1141.
15. D. Roy, W. L. Brooks, B. S. Sumerlin, *Chem. Soc. Rev.*, 2013, **42**, 7214.
16. M. T. Calejo, S. A. Sande, B. Nyström, *Expert Opin. Drug Deliv.*, 2013, **10**, 1669.
17. J. Ramos, A. Imaz, J. Forcada, *Polym. Chem.*, 2012, **3**, 852.
18. X. Xu, J. Song, K. Wang, Y. Gu, F. Luo, X. Tang, P. Xie, Z. Qian, *Macromol. Res.*, 2013, **21**, 870.
19. D.-W. Hong, P.-L. Lai, K.-L. Ku, Z.-T. Lai, I. M. Chu, *Polym. Degrad. Stab.*, 2013, **98**, 1578.
20. R. París, Á. Marcos-Fernández, I. Quijada-Garrido, *Polym. Adv. Technol.*, 2013, **24**, 1062.
21. S. T. Deshpande, S. R. Lahoti, D. L. Dhamecha, V. B. Rajendra, M. H. G. Dehghan, P. K. Puranik, *India J. Pharm. Educ. Res.*, 2013, **47**, 27.
22. J. I. Ngadaonye, L. M. Geever, M. O. Cloonan, C. L. Higginbotham, *J. Polym. Res.*, 2012, **19**, 1.
23. C.Y. Gong, S. Shi, L. Wu, M.L. Gou, et al, *Acta. Biomater.*, 2009, **5**, 3358.
24. Y. Yuan, Y. Cui, L. Zhang, H. P. Zhu, Y. S. Guo, B. Zhong, X. Hu, X. H. Wang, L. Chen, *Int. J. Pharm.*, 2012, **430**, 114.
25. E. Josef, K. Barat, I. Barsht, M. Zilberman, H. Bianco-Peled, *Acta Biomater.*, 2013, **9**, 8815.
26. M. Qiao, D. Chen, X. Ma, Y. Liu, *Int. J. Pharm.*, 2005, **294**, 103.
27. H. R. Lin, K. Sung, *J. Control. Release*, 2000, **69**, 379.
28. G. Lu, H. Jun, M. Dzimianski, H. Qiu, J. McCall, *Pharm. Res.*, 1995, **12**, 1474.

29. C. B. Liu, C. Y. Gong, M. J. Huang, J. W. Wang, Y. F. Pan, Y..D. Zhang, et al, *J. Biomed. Mater. Res. B*, 2008, **84**, 165.
30. C. Y. Gong, S. Shi, P. W. Dong, B. Yang, X. R. Qi, et al, *J. Pharm. Sci.*, 2009, **98**, 4684.
31. G. L. Ma, B. L. Miao, C. X. Song, *J. Appl. Polym. Sci.*, 2010, **116**, 1985.
32. X. W. Wei, C. Y. Gong, S. Shi, S. Z. Fu, et al, *Int. J. Pharm.*, 2009, **369**, 170.
33. C. Gong, S. Shi, P. Dong, B. Kan, M. Gou, X. Wang, X. Li, F. Luo, X. Zhao, Y. Wei, *Int. J. Pharm.*, 2009, **365**, 89.
34. G. Ma, B. Miao, C. Song, *J. Appl. Polym. Sci.*, 2010, **116**, 1985.
35. X. Wei, X. Lv, Q. Zhao, L. Qiu, *Acta Biomater.*, 2013, **9**, 6953.
36. C. Stein, M. J. Millan, A. Herz, *Pharmacol. Biochem. Behav.*, 1988, **31**, 445.
37. T. Mosmann. *J. Immunol. Methods*, 1983, **65**, 55.
38. S. Xu, R. Bian, X. Chen, Pharmacological experimental method. *People's Med Pub House, Beijing* 1991, 1424.
39. H. Devalapally, Z. Duan, M. V. Seiden, M. M. Amiji, *Int. J. Cancer*, 2007, **121**, 1830.
40. M. Li, Z. Tang, S. Lv, W. Song, H. Hong, et al, *Biomaterials*. 2014;**35**;3851.
41. S. J. Bae, J. M. Suh, Y. S. Sohn, Y. H. Bae, S. W. Kim, B. Jeong, *Macromolecules*, 2005, **38**, 5260.
42. P. Ferruti, I. Mancin, E. Ranucci, C. De Felice, G. Latini, M. Laus, *Biomacromolecules*, 2003, **4**, 181.
43. Y. Octavia, C. G. Tocchetti, K. L. Gabrielson, S. Janssens, H. J. Crijns, A. L. Moens, *J. Mol. Cell Cardiol.*, 2012, **52**, 1213.
44. O. Tacar, P. Sriamornsak, C. R. Dass, *J. Pharm. Pharmacol.*, 2013, **65**, 157.